Preseismic Fault Slip and Earthquake Prediction

J. H. DIETERICH

U.S. Geological Survey, Menlo Park, California 94025

It is proposed that preseismic fault creep may be the underlying process that is responsible for observations of earthquake precursors. The assertion that fault creep precedes earthquakes is supported by evidence from at least some earthquakes and by analogy with detailed laboratory observations. Laboratory observations of stick slip reveal that at least two stages of preseismic slip are an intrinsic part of the process leading to seismic slip on preexisting faults with inhomogeneous stress or strength. During the slowly propagating first stage of creep it is assumed that the length of the creeping fault segment is proportional to the source length of the subsequent earthquake. The data giving the well-known relationship between precursor time and earthquake magnitude are closely satisfied if the rate of propagation of the first stage of creep is independent of fault length. Long-term precursors may arise because of stress-strain variations during the first stage of fault creep. Observations of short-term precursors immediately prior to earthquakes may be related to the second short-lived state of preseismic fault slip seen in stick slip experiments.

INTRODUCTION

Anomalous changes of physical parameters prior to earthquakes have been reported in a variety of geological settings from different parts of the world. *Scholz et al.* [1973], *Whitcomb et al.* [1973], and *Mjachkin et al.* [1972] summarize many of these observations. Anomalous changes preceding earthquakes have been reported for apparent seismic velocity or travel times, crustal deformations, electrical resistivity, b values, magnetic field, groundwater chemistry, and water levels in wells.

A commonly stated characteristic of these observations is that the logarithm of the anomaly duration increases linearly with earthquake magnitude. This relationship has been advanced by *Scholz et al.* [1973], *Whitcomb et al.* [1973], and others. That such a variety of observations should obey the same law strongly suggests that the same overall process operates to control the variations of these parameters prior to earthquakes.

Most attempts to determine this mechanism have concentrated on observations of the ratio of compressional to shear velocity, V_p/V_s, prior to earthquakes. These observations, which have provided one of the most widely reported earthquake precursors, indicate that V_p/V_s first decreases to anomalously low values in advance of an earthquake and then recovers to approximately the normal values shortly prior to the earthquake. Theories that have been advanced to explain the V_p/V_s and other anomalies have placed a common emphasis on the importance of dilatancy.

Alone, dilational effects would seem to explain some but not all of the characteristics of the observations. For example, dilatancy would predict a progressive decrease in V_p/V_s as the shear stress increases to the critical level for failure, but it offers no explanation for the recovery of V_p/V_s prior to the earthquake.

Two substantially different hypotheses have arisen that attempt to combine dilatancy with other processes to explain the full details of the V_p/V_s variations and the other precursors observed. The diffusion-dilatancy hypothesis assumes that the opening of cracks and increase of pore volume induce fluid pressure variations and pore fluid migration. With this model, velocity recovery begins when the rate of water migration exceeds the dilational strain rates. Proponents of this theory [*Nur*, 1972; *Scholz et al.*, 1973; *Whitcomb et al.*, 1973] have argued that it predicts the observed characteristics of the precursor time versus magnitude data. The second hypothesis is really a collection of somewhat different models by *Mjachkin et al.* [1972], *Stuart* [1974], *Brady* [1975], and *Mogi* [1974] to explain velocity recovery without fluid diffusion in the focal zone. Although these models differ in many details, all share a common feature: earthquakes occur following a period of stress changes that characterize preseismic deformation. This change in stress is held to be caused by processes in the focal zone in preparation for the earthquake. Most theories call upon a preseismic drop in stress that results in a decrease of dilation strain and recovery of seismic velocity. A weakness of these models has been the failure to account specifically for the $\log t$ versus M relationship. Additionally, in the case of *Mjachkin et al.* [1972] and *Brady* [1975] the models are developed in terms of phenomena for the fracture of originally intact materials. The application of these models to repeated and frequent slip on existing faults has not been fully explored. The model proposed by Stuart is similar but recognizes the existence of a preexisting fault zone of weaker material. This model is general but nonquantitative and is expressed in terms of the constitutive laws for the fault zone and nearby rocks. The essential feature of this model is an accelerating anelastic deformation of the fault zone when the stress approaches some critical limit. This accelerating deformation in the fault zone causes the stresses to drop in the vicinity of the fault, reducing dilatancy and giving rise to an increase of seismic velocity. In this context, preseismic fault slip in the earthquake source region could be the mechanism for stress drop that results in velocity recovery.

Several authors cite evidence which suggests that preseismic fault slip has occurred before at least some earthquakes. At the Cienega Winery on the central California portion of the San Andreas fault, fault creep rates accelerated from 12 to 20 mm/yr 18 months prior to two earthquakes (M = 5.5 and 5.6) on April 9, 1961 [*Tocher*, 1960; *Nason and Tocher*, 1971; *Nason*, 1973]. At the time of these events, 11 mm of slip occurred at the winery. Two weeks prior to the M = 5.5, June 27, 1966, Parkfield, California, earthquake, *Allen and Smith* [1966] report that unusual ground cracking was observed that could have been caused by fault slip. *Yerkes and Castle* [1967] report that 9 hours before that same earthquake an irrigation pipeline crossing the fault ruptured because of accumulated fault slip.

Paper number 8B0294.

Both locations were on portions of the San Andreas fault that slipped at the time of the earthquake. *Stuart and Johnston* [1975] propose that tilt precursors beginning 6–16 days prior to five earthquakes M = 2.9–4.3 in central California can best be modeled by a double-couple source caused by preseismic slip at or near the earthquake source.

On a shorter time scale, *Kanamori and Cipar* [1974] conclude that very large preseismic slip amounting to 30-m displacement over a fault area of 200 × 800 km² began about 15 min prior to the M_s = 8.3 Chilean earthquake of May 22, 1960, but immediately following a magnitude 7.5 foreshock. Their analysis is based upon a very long period signal recorded on a strain seismograph prior to the main shock signal. Kanamori and Cipar also cite several cases of large-scale ground deformation occurring minutes to hours before earthquakes in Japan and suggest that these occurrences could also have been caused by premonitory fault slip. It seems likely that other such cases of shorter time scale crustal uplift prior to earthquakes could also be modeled by preseismic slip at or adjacent to the earthquake source.

This paper has two purposes. First, laboratory evidence for preseismic slip in artificially faulted samples will be presented. Second, it will be shown that mechanisms involving premonitory fault slip are compatible with the slope of the log t versus M data.

LABORATORY OBSERVATION ON PREMONITORY SLIP

Laboratory experiments on rocks containing artificial faults, either prepared saw cuts or induced fractures, have provided considerable insight into the mechanics of crustal earthquakes. In general terms, two types of slip behavior, stable sliding and stick slip, are widely recognized when progressively greater shear loads are applied to artificial faults. Stable sliding is characterized by the smooth displacement on the fault surfaces without sudden changes in the displacement rate. Under uniform rates of loading the slip rates ideally remain constant. Stick slip is the unstable episodic sliding of a fault. Ideally, a stick slip cycle consists of a relatively long period in which no slip takes place and the shear stress increases, punctuated by the abrupt onset of rapid slip accompanied by a stress drop. There is good evidence that the instability process associated with laboratory stick slip is related to, if not the same as, the instability process that controls shallow earthquakes on faults [*Brace and Byerlee*, 1966; *Scholz et al.*, 1972; *Dieterich*, 1974]. Similarly, stable sliding has often been equated with aseismic fault creep.

For stick slip, detailed observation of the loading cycle preceding rapid slip has shown that rarely, if ever, does the actual process conform to the ideal case outlined above. A number of investigations [*Byerlee*, 1967; *Logan et al.*, 1972; *Scholz et al.*, 1972] have demonstrated that small amounts of slow aseismic slip occur during the late stages of the loading cycle that precedes rapid slip.

Scholz et al. examined the details of premonitory creep on ground surfaces of Westerly granite subjected to biaxial loading at stresses normal to the slip surface to 100 MPa. In these experiments they found that small amounts of stable sliding with accelerating rates of slip preceded virtually all stick slip events. The amounts of slip were small, of the order of 5–15 μm, and amounted to 2–5% of the slip in the subsequent stick slip event. At loading rates of 7×10^{-8} s^{-1} to 7×10^{-6} s^{-1} the amount of premonitory slip and the form of the time versus displacement curve were relatively unchanged. The onset of premonitory slip began in the last 25% of the loading cycle.

Byerlee and Summers [1975] have examined premonitory slip under different experimental circumstances. Here, jacketed, initially intact cylindrical samples of Westerly granite under confining pressures to 6 kbar were first fractured to produce artificial faults. Friction experiments were then conducted on the faulted specimens. Premonitory displacements varied from ~0.01 to 2.5 mm and showed a systematic variation with confining pressures. Maximum premonitory slip was observed at low confining pressures, and the minimum at the high confining pressures. As in the case of the Scholz et al. experiments, they have suggested the possibility that stable fault slip may precede earthquakes.

For the extrapolation to earthquake faults the above data permit two interpretations that lead to drastically different conclusions. First, the amount of preseismic slip may be independent of fault dimensions if it is controlled by local, size-independent material properties. Hence preseismic slip displacements could be of similar magnitude for laboratory specimens and large faults. If this is the case, then premonitory slip would be difficult to observe and would not be of significance.

Second, premonitory displacements may be proportional to slip-induced stress or strain changes on the fault. In this case, scaling requires that stress or strain changes be proportional to displacement divided by fault dimensions. Hence displacements would be proportional to fault dimensions, and significant displacements could occur prior to earthquakes. Recently, laboratory experiments have been conducted that provide added information and better insight into the process of premonitory slip. These results do not conclusively resolve the scaling question but can best be interpreted as indicating that premonitory displacements are proportional to fault length.

The experimental configuration is illustrated in Figure 1. A block of Westerly granite with dimensions of 127 × 127 × 40 mm was loaded biaxially with hydraulic rams acting parallel to the two major dimensions of the sample. Slip takes place on a carefully resurfaced and well-mated saw cut oriented at 45° to the two load axes. Profilometer readings obtained directly from the surface gave an average peak-to-trough roughness of 2×10^{-1} μm with occasional pits to 9×10^{-1} μm deep at a minimum measured wavelength of 20 μm. Semiconductor strain gages at 16 locations on the sample provide detailed information on the strain state adjacent to the artificial fault.

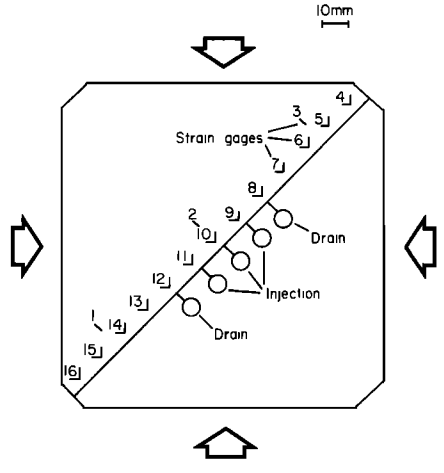

Fig. 1. Sample configuration showing locations of strain gages. Gages 1–3 give normal strains, and gages 4–16 give shear strains parallel to the fault.

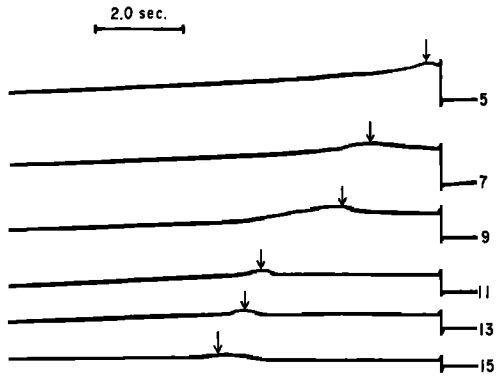

Fig. 2. Slow-speed oscillograph record of stick-slip event showing large amounts of slowly propagating preseismic slip. Numbers refer to gage locations. Arrows mark the time at which fault slip began at each strain gage.

Thirteen of these strain gages record shear strains parallel to the surface, and the remaining three gages give strains normal to the surface as shown in Figure 1. Five holes were drilled in the sample to permit fluid injection/withdrawal on the fault surface. The purpose of this arrangement was to limit the dimensions of the slip zone by locally altering the effective normal stress. For the results presented here the injection holes were not in operation.

Experiments were conducted at low normal stresses in range 4–18 MPa. Stick slip was observed throughout this range. Of more than 150 stick slip events recorded in detail, premonitory slip was observed in all but two cases.

Figures 2 and 3, which are oscillograph recordings of shear strains at low speed and high speed, respectively, show the principal characteristics of recorded premonitory creep events. A decrease of amplitude of the curves corresponds to a drop of shear stress and is caused by slip on the fault immediately ajacent to the gages. Increases of shear stress are caused by increases in the externally applied load and by stress concentrations that arise from slip on nearby portions of the fault. In Figures 2 and 3, arrows mark the times at which slip first begins.

Figure 2 illustrates a feature that seems to be characteristic of most events—slip begins at some point on the fault and slowly propagates over a significant fraction of the surface prior to unstable slip. At higher recording speeds (Figure 3), two added characteristics become evident. First, an additional, more rapidly propagating preseismic slip event can be recognized. Second, the seismic slip event appears to begin at an identifiable point on the fault as an acceleration of the local slip rate. The unstable slip event then propagates outward from this point at a rapid velocity.

For the events illustrated by Figures 2 and 3 it would appear that slip proceeded very slowly until the slip event reached the edge of the sample, seismic slip occuring shortly thereafter. At high recording speeds (Figure 3) it is seen that a second and more rapid event began to propagate from that end toward the middle of the sample. At gage 10 this more rapid slip smoothly accelerates to become part of the seismic slip event. Seismic slip in turn propagated bilaterally at a high velocity (~1.5 km/s) from point 10.

Although the individual stick slip events are highly variable in detail, slip for most events can be divided into three distinct stages. Stage I is the slow propagation of slip across the sample, with slip rates controlled by the externally applied rate of displacement used to load the sample. These observations and the observation by *Scholz et al.* [1972] that the form of the preseismic slip displacement-time curve and magnitude of slip are independent of experimental loading rate suggest that stage I slip is a stable process that is driven by the external loading. Stage II consists of a much shorter interval ($<10^{-2}$ s) after the initial slip event reaches the sample edge. The shear stress decreases during stage II. It is worth emphasizing perhaps that the second stage of slip was repeatedly observed and appears to consist of a slip velocity perturbation triggered when the stage I slip breaks out at the end of the sample. During stage II the propagation of accelerated slip back through the specimen is driven by the stored elastic strain. The process appears to be intrinsically unstable. At first the slip appears to be overdamped, and the slip velocities remain low with only a minor decrease in the frictional force. As the boundary of the accelerated slip zone moves back through the sample, the decrease in frictional resistance and the increase of slip rate behind the boundary increase the rate of elastic strain loading at the front of the boundary. As a result the onset of accelerated slip at the advancing boundary is associated with an increasingly larger step in slip velocity and larger drop in frictional force across the slip surface. At some point the frictional damping of the propagating boundary becomes insufficient to stabilize the process, and the slip boundary propagates at near seismic speeds. Stage III is the resulting unstable (seismic) slip that is driven by a sharp drop in frictional force. For these experiments the fractional stress drop $\Delta\tau_s/\tau$ for

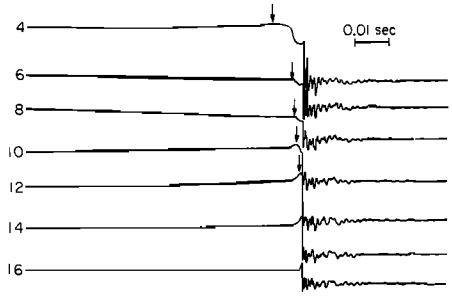

Fig. 3. High-speed oscillograph record of stick slip event. Not shown on this record because of the short time scale is the initial slowly propagating slip event that has already transversed the sample from bottom to top. Arrows mark the propagation of the second, more rapidly propagating preseismic slip event. Note that at gages 10 and 12 the seismic slip is transitional with preseismic slip. Oscillations following the stress drop are caused by vibration of the loading frame.

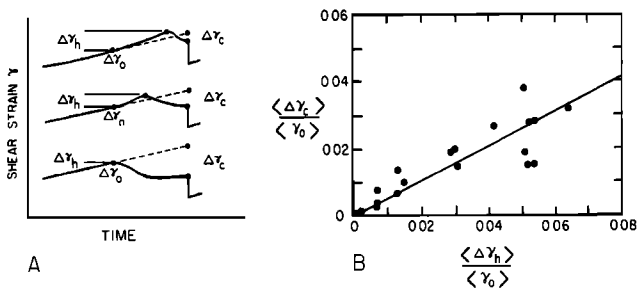

Fig. 4. Effect of heterogeneity on stage I slip. (*a*) Schematic diagram of shear strains recorded by the strain gages plotted against time. Slip first begins at time t_0, when the local strains are γ_0. Illustrated for each gage are $\Delta\gamma_c$, the strain caused by preseismic slip, and $\Delta\gamma_h$, the critical strain required to initiate slip measured in relation to γ_0. (*b*) Data for the amount of preseismic slip against heterogeneity; $\langle\Delta\gamma_c\rangle$ and $\langle\Delta\gamma_h\rangle$ are the average values of $\Delta\gamma_c$ and $\Delta\gamma_h$ from all gages showing stage I slip. The data are normalized by $\langle\gamma_0\rangle$, the average shear strain at the time that slip begins.

stage III slip has an average value of 0.09, where $\Delta\tau_s$ is the change in shear stress for stick slip and τ is the shear stress immediately prior to seismic slip.

The extensive use of strain gages brought to light an added characteristic of these experiments that is probably common to all friction experiments and faulting in general. It was found that upon loading the sample the shear stresses/strains were not uniform but varied considerably and in a somewhat unpredictable fashion. Largely by trial and error it was found that the inhomogeneity of stress/strain could be reduced by realigning the sample within the apparatus and by using cardboard wafers of various thicknesses between the steel bearing plates and the sample. By changing the variability of shear stresses in this fashion it was found that the amount of premonitory slip changes also. Figure 4 summarizes the results of a series of experiments with differing levels of heterogeneity of the shear strain. These data were obtained from slower-speed recordings and therefore give strain changes for only the first stage of preseismic slip. The method of defining heterogeneity and preseismic slip is illustrated by Figure 4*a*, which schematically shows the characteristic features of individual shear strain records. Heterogeneity $\langle\Delta\gamma_h\rangle$ is defined as the average of differences between the shear strain when slip first begins at some point in the sample and the critical shear strain required to initiate slip locally, measured at each strain gage that shows preseismic slip. As a measure of the magnitude of preseismic slip the quantity $\langle\Delta\gamma_c\rangle$ is taken to be the average difference between the observed shear strain at the time seismic slip begins and the shear strain extrapolated from the loading paths prior to the initiation of stage I slip. The data in Figure 4 are normalized by $\langle\gamma_0\rangle$, the average total shear strain at the time t_0 when stage I slip first begins. Those data imply the empirical relationship for stage I slip propagation:

$$\langle\Delta\gamma_c\rangle/\langle\gamma_0\rangle = K\langle\Delta\gamma_h\rangle/\langle\gamma_0\rangle \quad (1)$$

The solid line in Figure 4*b* is a linear least squares fit to the data that passes through the origin. The slope, K, has the value 0.52. Taking shear stress to be proportional to shear strain in (1) gives

$$\langle\Delta\tau_c\rangle = K\langle\Delta\tau_h\rangle \quad (2)$$

where $\langle\Delta\tau_h\rangle$ is the average change in shear stress required to overcome the fault friction measured in relation to the shear stress when slip first begins and $\langle\Delta\tau_c\rangle$ is the average total change in shear stress caused by preseismic slip measured in relation to the stresses extrapolated to the time when seismic slip begins.

The data of Figure 4*b* show that reduction of the difference between the applied shear strain and the critical strain required to initiate slip results in a reduction of the magnitude of preseismic slip. Corresponding changes in the duration of slip and the velocity of propagation of the slip front are also observed. Hence a decrease in $\langle\Delta\gamma_h\rangle$ results in a decrease of the duration of slip and an increase of propagation velocity. For two events arranged to give minimum heterogeneity, no stage I slip preceded stages II and III. These observations suggest that stage I slip is stable because the extension of the stage I slip area is driven against some sort of stress gradient which is measured by $\langle\Delta\gamma_h\rangle$. Hence an increment of boundary displacement is required to initiate an increment of slip area extension.

The strain versus time records indicate that preseismic slip takes place at approximately constant local stress while the increase of stress on the stationary portions of the fault is controlled by the loading rate, R. Hence during the growth of the slip area,

$$\langle\Delta\tau_c\rangle \sim Rt \quad (3)$$

where t is the duration of slip. The region undergoing slip, L, enlarges at velocity V. In many cases (e.g., Figure 2), V is approximately constant:

$$L \sim Vt \quad (4)$$

If S is the gradient of the difference between the critical stress for slip and the applied stress, then

$$L \sim (1/S)\Delta\tau_c \quad (5)$$

It will be noted that S is proportional to $\langle\Delta\tau_h\rangle$. Combining (3), (4), and (5) gives

$$V \sim R/S \quad (6)$$

which is in qualitative agreement with the observations noted above.

Fault displacements were not measured in these experiments. However, some characteristics of the displacement history can be inferred from the strain versus time records. As the length of the zone of stage I slip enlarges, an estimate of the displacement D may be obtained by using the conventional dislocation-fault length relationship for an elastic body:

$$D = (\eta/\mu)L\langle\Delta\tau_c\rangle \quad (7)$$

where μ is the shear modulus and η is a geometric factor with values near 1 [*Chinnery*, 1967]. Combining with (4), (5), and (6) gives

$$D \sim (\eta/\mu)RVt^2 \quad (8)$$

Hence fault displacement D increases by t^2 as the slip area increases in size. This result is in qualitative agreement with the *Scholz et al.* [1972] observations, which show a roughly exponential acceleration of preseismic displacements. It would appear therefore that the form of the displacement-time curves measured by *Scholz et al.* [1972] reflects the growth of the area of preseismic slip.

The dependence of the amount of stage I slip on levels of inhomogeneity of stress along the fault is similar to the 'priming' of a fault as postulated by *Weertman* [1964] and may be analogous to observations on the effect of material heterogeneities on earthquake b values in simulations with deterministic numerical models and for microshock b values in laboratory experiments. In a series of laboratory experiments with different materials, *Mogi* [1967] has shown that value of b is controlled by material heterogeneities. The greater the heterogeneity, the greater b, and hence the greater the energy dissipation by small shocks relative to large shocks.

Similar results are obtained with a one-dimensional numerical analog of an earthquake active fault as described by *Dieterich* [1972]. With these models, variations of strength with location on the fault provide the heterogeneity necessary to limit the dimensions of earthquake ruptures. Without some heterogeneity, slip would always take place over the entire length of the fault. The heterogeneity acts to establish barriers of variable height, where the initial shear stress is less than the strength. On a fault with suitable heterogeneity a large earthquake occurs only after smaller earthquakes have taken place. The smaller shocks play an essential preparatory role for the large shocks by increasing the shear stress on the stronger portions of the fault and hence reducing the effective height of the barriers. When the relative height of the barriers is suf-

ficiently reduced, a throughgoing rupture is then able to develop. The greater the height of the barriers, the greater the number of preparatory events.

The data given in Figure 4 suggest a similar interpretation for premonitory slip. Seismic slip in the absence of premonitory creep occurred only when the barriers, i.e., stress inhomogeneities, were very small. In the usual situation, where seismic slip occurs following fault creep, the heterogeneity on the fault at the time of unstable slip is also effectively zero. It is concluded therefore that preseismic slip plays an essential preparatory function for seismic slip by reducing the effective barrier height. Stages II and III occur only when the stresses are at or very near the critical stress required to sustain fault creep. During stage I the slip area grows only when the stress concentrations at the edges of the slipped zone overcome the barriers. Stresses at the ends of the zone increase when the displacement on the slipped segment increases. The higher the barriers, the greater the slip required to produce the necessary stress concentration to allow propagation.

At this juncture, two questions relevant to the application of preseismic slip to earthquake faults may be asked. First, what is the magnitude of $\langle \Delta\tau_h \rangle$ for faults? Second, is it possible that preslip occurs on very limited portions of a fault and that seismic slip propagates well beyond the preslip zones? The latter question would appear to be a fundamental uncertainty in applying preseismic slip mechanisms to earthquake precursors. If dimensions of the zone of preseismic slip are small and unrelated to the final size of the earthquake source, it becomes unlikely that this mechanism could explain the various earthquake precursor observations discussed earlier or that preseismic slip could ever be useful for prediction of earthquakes. In the absence of definitive evidence and for the purpose of developing the following discussion it is argued that earthquake faults have a higher level of heterogeneity than the finely surfaced laboratory samples which have been studied and that the dimensions of the zone of preseismic slip are comparable to the dimensions of the earthquake source.

Indirect evidence supporting these assumptions is given by the absence of observations of self-contained slip events in the experiments just described. The detailed coverage of the slip surface with strain gages permits recognition of slip events with dimensions as small as $\sim\frac{1}{8}$ that of the entire slip surface. Only when the effective heterogeneity of the surface was increased by locally injecting fluid onto the surface were confined slip events produced. Because heterogeneity of earthquake active faults limits the dimensions of seismic slip, it appears likely therefore that the values of $\langle \Delta\gamma_h \rangle$ measured for the laboratory experiments in Figure 4 are less than those for faults. In turn, high values of heterogeneity on active faults will tend to reduce the possibility of 'runaway' earthquakes in which seismic slip propagates well beyond the zone of preseismic slip. This is because higher relative values of heterogeneity outside the preseismic slip zone will impede seismic slip.

The following discussion assumes that possible long-term precursors originate because of stress or strain changes in the source region caused by preseismic fault creep. *Mjachkin et al* [1972], *Stuart* [1974], and *Brady* [1975] discuss some possible mechanisms by which reported precursors may be explained by preseismic deformations.

DURATION OF ANOMALIES

A number of investigators have reported a correlation between M and duration of the anomalous period t (Figure 5). The empirically determined relationship is of the form

$$M = \alpha + \beta \log t \tag{9}$$

Scholz et al. [1973] give values for $\alpha = -5.81$ and $\beta = 1.55$, and *Whitcomb et al.* [1973] give two sets of values, $\alpha = -5.33$, $\beta = 1.47$; and $\alpha = -3.77$, $\beta = 1.25$, respectively, for time measured in seconds. The data for this correlation are as yet poorly established, and therefore (9) should be regarded with some caution. However, if it is assumed that future observations will support this correlation, then (9) obviously provides important constraints on the mechanical processes controlling earthquake precursors.

Aggarwal et al. [1973], *Scholz et al.* [1973], and *Whitcomb et al.* [1973] compare t to earthquake source length L. Because $\log L$ is proportional to M, a relationship of the form $t \sim L^n$ is to be expected from (9). Aggarwal gives a value of $n = 1.6$, and *Scholz et al.* [1973] and *Whitcomb et al.* [1973] find a value of $n \sim 2.0$. An impressive argument favoring dilatancy-diffusion has been the prediction of $n = 2.0$ by that model.

Heretofore, the diffusionless models have not offered a specific explanation of the observed dependence of t on M. *Anderson and Whitcomb* [1975], however, have argued that the observations on precursor times are not necessarily unique to a diffusion mechanism. They find empirically that the time interval t_l separating earthquakes of a given magnitude and characteristic dimension L is given by

$$t_l \sim L^2 \tag{10}$$

On the basis of a similarity argument for stress-strain behavior, Anderson and Whitcomb conclude that if t_l is proportional to L^2, then the onset times for other stages in the stress-strain cycle such as the beginning of dilatant behavior should also scale by L^2—quite independent of water diffusion. It might follow then from this line of reasoning that precursor times for mechanisms involving preseismic slip could also scale by L^2. However, I believe that this result is erroneous because of a misapplication of (10). Also, it appears that the data used to establish the L^n dependence of precursor time contain such large possible uncertainties so as to preclude a definitive determination of $n = 2$. Each of these points will be discussed in turn.

To derive (10), Anderson and Whitcomb employ the magnitude-frequency relationship

$$\log N = a + bM \tag{11}$$

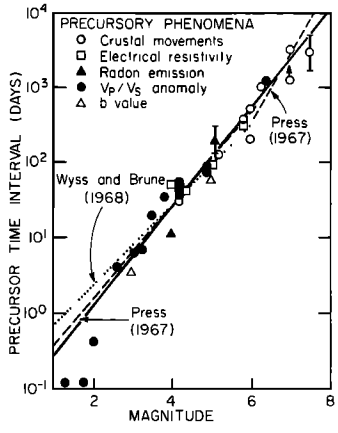

Fig. 5. Earthquake precursor time versus magnitude [from *Scholz et al.*, 1973]. Solid line is the *Scholz et al.* [1973] fit to the data, and dashed and dotted curves are fits to these data based on (19), using the magnitude-fault length relationships of *Press* [1967] and *Wyss and Brune* [1968], respectively.

with the aftershock area-magnitude relationship

$$\log L^2 = c + M \tag{12}$$

giving

$$\log N = a - bc + b \log L^2 \tag{13}$$

where N is the number of earthquakes of magnitude M, L^2 is the aftershock area characteristic of M, and a, b, and c are constants with $b \sim -1$. Taking $N = n/t$, where n is the number of shocks per unit time, it follows that recurrence time

$$\log t_t = -a - c + \log L^2 \tag{14}$$

or $t_t \sim L^2$. The recurrence interval t_t applies to earthquakes with fault area L^2 taking place within a region which has a total seismically active fault area of L_t^2. It is not the recurrence time for slip on a specific fault segment of area L^2. This is because in general, $L_t^2 \neq L^2$. For example, in the usual case when $L_t^2 >> L^2$ there will be many subregions with fault area L^2 that are simultaneously undergoing the stress-strain path leading to earthquakes of magnitude M. The time t_t is clearly the interval between events of magnitude M occurring in all the different subregions. It is not the interval between successive seismic events with area L^2 occurring within a given subregion of the same size and therefore should not be applied directly to obtain the time for the stress-strain cycle of that subregion. Taking t_t' as the recurrence time for slip on subregion L^2, the ratio of t_t' to t_t is given by the ratio of L^2 to L_t^2:

$$t_t'/t_t + L_t^2/L^2 \tag{15}$$

Substituting t_t from (15) into (14) gives

$$\log t_t' = -a - c + \log L_t^2 \tag{16}$$

Hence to a first approximation the recurrence interval for slip on a fault segment of area L^2 is independent of the magnitude of L.

On examination this result appears to be reasonable. Consider, for example, an idealized stress cycle consisting of a uniform stress buildup that begins immediately following an earthquake and culminates with a stress drop at the time of the next earthquake. Data for earthquake stress drops show considerable scatter but usually fall in the range 0.1–10 MPa with scant indication of a regular variation with magnitude (see, for example, the data of *Thatcher and Hanks* [1973] and *Chinnery* [1967]). If there is a magnitude dependence in the range M = 2–8, it must certainly be very weak. The result (equation (16)) implies that t_t' is independent of L^2, and since stress drop is also independent of L^2, then the rate of stress increase between earthquakes must also be independent of L^2; i.e., the rate of tectonic loading on a fault is independent of the size of the segment being examined.

On the other hand, a possible $t_t' \sim L^2$ dependence requires that either the rate of loading scale by L^{-2} if earthquake stress drops are held to be independent of size or that the stress drop must be proportional to L^2 if the rate of stress increase is independent of size. The former case implies that tectonic loading somehow depends on the size of the region being examined, while the latter case requires that stress drops for earthquakes in the range M = 2–8 vary by about 8 orders of magnitude.

As it pertains to the empirical determination that $n = 2$ in the relation $t \sim L^n$ by *Scholz et al.* [1973] and *Whitcomb et al.* [1973], the position is taken here that large possible uncertainties in that data set preclude a definitive determination of n. The finding $n = 2$ (Figure 6) is based on far fewer observations than the magnitude versus precursor time relationship, which is poorly established itself and is sensitive to any uncertainties of a relatively small number of data points. Additionally, the data for L have been obtained only partially from direct observations. For most of the larger earthquakes, L seems to have been obtained from the dimensions of the aftershock zone, while for the smaller earthquakes (from Blue Mountain Lake, New York, and Garm, Tadjikistan), *Whitcomb et al.* [1973] employed the *Wyss and Brune* [1968] empirical relationship for magnitude and length. The determination of slope of the L versus t curve depends greatly on these smaller earthquakes and is therefore sensitive to the parameters of the Wyss and Brune relationship or to errors in earthquake locations if size of aftershock zone is employed. To illustrate the possible uncertainty in the determination of L using empirical magnitude-length relationships, the New York and Tadjikistan earthquakes have been replotted by using the *Press* [1967] relationship for small earthquakes (open circles in Figure 6). Use of the open circles tends to reduce n to a value nearer 1.0. Finally, the lengths and precursor times extrapolated to very large earthquakes by using the Whitcomb et al. data (Figure 6) seem incompatible with the more extensive data for source parameters and precursor time versus magnitude (Figure 4). For example, at M = 8 the t versus M curve of Scholz et al. predicts $t = 10^4$ days, while Whitcomb et al. predict $t = 3 \times 10^4$ and 1.4×10^4 days (vertical bar in Figure 6). From study of source parameters of large earthquakes [*Tocher*, 1958; *Iida*, 1965; *Press*, 1967] it is known that at M =

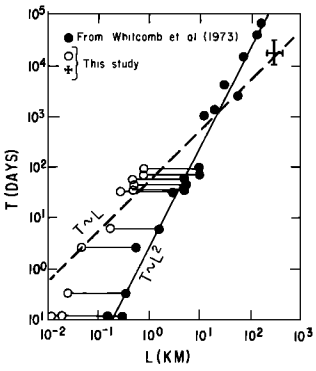

Fig. 6. Earthquake precursor time versus fault length (data modified after *Whitcomb et al.* [1973]). Solid circles are from *Whitcomb et al.* [1973]. Open circles give length determinations based on the *Press* [1967] *M-L* relationship for intermediate and small earthquakes instead of the *Wyss and Brune* [1968] relationship employed by *Whitcomb et al.* [1973]. The cross represents possible range of t and L for M = 8 (see text).

TABLE 1. Predicted Values of β and Propagation Velocities From Magnitude-Length Scaling Equation

$\beta = B$	V,* cm/s	Magnitude-Length Relationship
	$M < 6$	
1.6	2.1×10^{-2}	*Press* [1967]
1.9	1.9×10^{-2}	*Wyss and Brune* [1968]
	$M \geq 6$	
0.98	1.2×10^{-2}	*Tocher* [1958]
0.76	8.6×10^{-3}	*Iida* [1965]
1.06	1.3×10^{-2}	*Press* [1967]

*Velocities are obtained from the best fit to Scholz et al. *M-t* data.

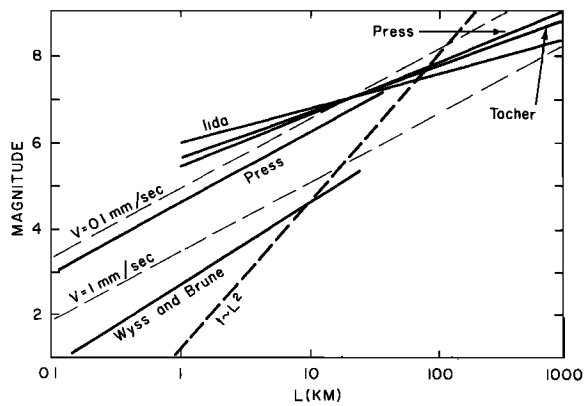

Fig. 7. Magnitude-length relationship from *Press* [1967], *Wyss and Brune* [1968], *Tocher* [1958], and *Iida* [1965]. Dashed curves are magnitude-length relationships and stage I propagation velocities that exactly satisfy the *Scholz et al.* [1973] fit to the *M-t* data (Figure 6), under the assumption that $t \sim L^1$ in (17)–(20). The heavy dashed curve is an exact fit assuming $t \sim L^2$ instead of (17).

8, L will fall in the range 200–400 km (horizontal bar in Figure 6). Taking L = 300 km, the L versus t curve of *Whitcomb et al.* [1973], however, gives a precursor time of 2×10^6 days, an order of magnitude discrepancy with the M versus t data. A reviewer has pointed out the probable explanation for this discrepancy: the three largest earthquakes are from *Tsubokawa* [1969] and properly represent recurrence times and not precursor times.

Premonitory slip as treated here seems to be most compatible with a $t \sim L$ dependence (equation (4)). In order to derive relationships of the form of (9) it is assumed that stage I preseismic slip takes place over some fault length l, which is proportional to the earthquake source dimension L. For simplicity, l is taken equal to L. It is further assumed that the velocity of propagation V of the slip area is independent of L. Hence

$$t = L/V \tag{17}$$

On the basis of the above discussion of experimental data for stage I slip, (17) implies that loading rates and fault heterogeneity are comparable for all earthquakes. For most earthquakes which occur at plate margins, one might expect loading rates to be similar. Notable exceptions might include aftershocks where high apparent loading rates would be expected and intraplate earthquakes where rates may be significantly less than they are at plate margins.

Length parameter L may be related to M by using the conventional empirical relationship which has the form [*Chinnery*, 1969]

$$M = A + B \log L \tag{18}$$

Combining (17) and (18) gives

$$M = A + B \log V + B \log t \tag{19}$$

which is the same form as (9) with

$$\alpha = A + B \log L \qquad \beta = B \tag{20}$$

Values of B from *Press* [1967] and *Wyss and Brune* [1968] which are appropriate to moderate and small earthquakes are 1.60 and 1.89, respectively. Using L versus M data for large earthquakes [*Press*, 1967; *Tocher*, 1958; *Iida*, 1965] gives values for B from 1.06 to 0.98. See Table 1 and Figure 5 for comparison of data for (9) and (19). These results compare well with reported values of β from 1.25 to 1.55. Figure 7 plots data for (19). The dashed curves in Figure 7 give magnitude-length relationships that exactly satisfy the parameters for the *Scholz et al.* [1973] fit to the magnitude-time data. The heavy dashed curve in Figure 7 gives the slope of magnitude-length relationships with precursor times proportional to L^2 that would exactly satisfy the *Scholz et al.* [1973] magnitude–precursor time data.

An alternative to using the empirical M versus L relationships of (18) is to employ scaling laws for seismic energy and length in conjunction with empirical relationships for M and seismic energy. Dimensional analysis [*Dieterich*, 1973, 1974] requires

$$E = \frac{k}{\mu} L^3 \Delta\tau_s^2 \tag{21}$$

where E is seismic energy, k is constant with values near 1.0, and $\Delta\tau_s$ is the seismic stress drop. The relationship between earthquake energy and magnitude is generally approximated by

$$M = c + d \log E \tag{22}$$

Combining (21) and (22) and taking $t = L/V$ give

$$M = c + d \log \frac{k}{\mu} \Delta\tau_s^2 + 3d \log V + 3d \log t \tag{23}$$

or

$$M = \alpha + \beta \log t$$

with

$$\alpha = c + d \log \frac{k}{\mu} \Delta\tau_2 + 3d \log V \qquad \beta = 3d \tag{24}$$

From (24) the predicted values for $3d$ obtained from representative magnitude-energy relations (Table 2) are in the range 1.4–2.1. This result seems to be in reasonable agreement with the reported values of β = 1.25–1.55.

SUMMARY AND DISCUSSION

In summary the following are observed: (1) there is evidence that suggests significant amounts of preseismic slip for a few earthquakes, (2) preseismic slip on laboratory faults is an intrinsic part of the process of homogenization of stress along a fault leading to unstable (seismic) slip, and (3) a precursor time scaling relationship of $t \sim L$ is indicated by empirical magnitude-length and magnitude-precursor time relationships. That scaling is compatible with precursor models in which precursor time is controlled by the duration of propagating preseismic slip events. However, at present it cannot be definitely established that all or even many earthquakes have

TABLE 2. Predicted Values for β From Magnitude-Energy Scaling (Equations (20) and (21))

$\beta = 3d$	Magnitude-Energy Relationship
1.4	*King and Knopoff* [1969]
1.5	*Thatcher and Hanks* [1973]
1.6	*DeNoyer* [1959]
1.7	*Benioff* [1955]
2.0	*Gutenberg and Richter* [1956]
2.1	*Bath* [1958]

significant amounts of preseismic slip over source areas comparable to the characteristic area of the seismic source.

The following comments represent an initial attempt to outline a model for earthquake instability. The instability model derives its basis from experimental observations on effects of fault heterogeneity and two stages of preseismic slip.

Finite dimensions of earthquakes arise because of slip-limiting stress/strength variation on faults. These irregularities control the location and dimensions of earthquakes and must therefore exist over the full range of dimensions that characterize earthquakes of all magnitudes. Because irregularities in laboratory samples are generally insufficient to limit slip propagation, it appears that larger irregularities of stress and strength exist on natural faults. High levels of fault heterogeneity reduce the likelihood that seismic slip can propagate appreciably beyond the zone where preseismic slip has effectively reduced the heterogeneity; i.e., except for the maximum earthquake, when the entire fault slips, there is always an adjacent heterogeneity that has not yet been leveled out by preseismic slip.

By analogy with the laboratory observations it is proposed that preseismic fault slip takes place in two stages. The first stage consists of the long-term stable propagation of slip along the fault. The second stage is the shorter interval of accelerated slip that culminates in seismic instability.

Rate of loading and the inhomogeneity of stress/strength control the stage I slip and propagation velocity according to (1)–(8). Stage I slip serves to reduce the effective magnitude of stress inhomogeneity by overcoming the slip-inhibiting zones on the fault, where stress is less than the local frictional strength. Within the zone of stage I slip the shear stress is everywhere equal to the frictional strength of slow velocity slip. Therefore the effective barrier height is zero, and there is potential for seismic slip.

Stage II, the short interval of accelerated slip that culminates in seismic slip, is believed to underlie observations of short-term precursors such as that reported by *Kanamori and Cipar* [1974] for the May 22, 1960, Chile earthquake. In laboratory experiments (Figure 3), frictional resistance and hence stress decrease as slip velocity increases during stage II. The decrease of stress within the stage II zone of slip causes a rapid transfer of stress to the ends of the propagating stage II zone and therefore permits accelerated slip to propagate rapidly without added loading. In most cases, for these experiments, stage II slip did not propagate over the entire fault surface before the initiation of seismic slip. The interval from the beginning of stage II to the onset of seismic slip was usually from 0.001 to 0.01 s. This corresponds to propagation velocities of approximately 2×10^4 to 2×10^5 cm/s. An explanation for the mechanisms that control stage I slip cannot be offered at this time. However, an estimate of the upper limit for the duration of stage II for earthquakes can be made if it is assumed that propagation velocities are independent of scale or experimental conditions and that stage II slip propagates across the entire seismic source area. On this basis the maximum expected duration of accelerated preseismic slip for the 800-km source length of the May 22, 1960, Chile earthquake would be 67–670 min. For comparison the analysis of *Kanamori and Cipar* [1974] places the beginning of rapid preseismic slip approximately 15 min prior to the earthquake.

Stage II slip in the laboratory experiments was observed to begin as a velocity perturbation originating at the end of the sample at the time that stage I slip propagation reached that end. If the analogy with the laboratory experiments is continued for earthquakes on preexisting faults, then stage II slip would be expected to begin at the point of a local acceleration of slip.

It has been proposed that stage I slip events cause stress or strain changes in the source region that may in turn give rise to the earthquake percursors summarized in Figure 5. If reports of preseismic velocity anomalies and other precursors are borne out, precursor models incorporating preseismic slip would appear to warrant more detailed quantitative study.

Acknowledgments. Jerry Eaton and Barry Raleigh read the manuscript and suggested a number of improvements. Several aspects of this study were stimulated by discussions with Robert Nason, William Stuart, and Barry Raleigh.

REFERENCES

Aggarwal, T. P., L. R. Sykes, J. Armbruster, and M. L. Sbar, Premonitory changes in seismic velocities and prediction of earthquakes, *Nature, 241,* 101–104, 1973.

Allen, C. R., and S. W. Smith, Pre-seismic and post-earthquake surficial displacements, *Bull. Seismol. Soc. Amer., 56,* 966–967, 1966.

Anderson, D. L., and J. H. Whitcomb, Time-dependent seismology, *J. Geophys. Res., 80,* 1497, 1975.

Bath, M., The energies of seismic body waves and surface waves, in *Contributions in Geophysics in Honor of Beno Gutenberg,* Pergamon, New York, pp. 1–16, 1958.

Benioff, H., Seismic evidence for crustal structure and tectonic activity, *Geol. Soc. Amer. Spec. Pap., 62,* 61–73, 1955.

Brace, W. F., and J. D. Byerlee, Stick-slip as a mechanism for earthquakes, *Science, 153,* 990, 1966.

Brady, B. T., Theory of earthquakes, II, Inclusion theory of crustal earthquakes, *Pure Appl. Geophys., 113,* 149–168, 1975.

Byerlee, J. D., Frictional characteristics of granite under high confining pressure, *J. Geophys. Res., 72,* 3639–3648, 1967.

Byerlee, J. D., and R. Summers, Stable sliding preceding stick-slip on fault surfaces in granite at high pressure, *Pure Appl. Geophys., 113,* 63, 1975.

Chinnery, M. A., Theoretical fault models, Symposium on Processes in the Focal Region, edited by K. Kasahera and E. Stevens, pp. 211–223, *Publ. 34,* Dominion Observ., Ottawa, Ont., 1967.

Chinnery, M. A., Earthquake magnitude and source parameters, *Bull. Seismol. Soc. Amer., 59,* 1969–1982, 1969.

DeNoyer, J., Determination of the energy in body and surface waves, II, *Bull. Seismol. Soc. Amer., 49,* 1–10, 1959.

Dieterich, J. H., Time-dependent friction as a possible mechanism for aftershocks, *J. Geophys. Res., 77,* 3771–3781, 1972.

Dieterich, J. H., A deterministic near field source model, Proceedings of the Fifth World Conference on Earthquake Engineering, Rome, *Pap. 301,* 13 pp., 1973.

Dieterich, J. H., Earthquake mechanisms and modeling, *Annu. Rev. Earth Planet. Sci., 2,* 275–301, 1974.

Gutenberg, B., and C. F. Richter, Magnitude and energy of earthquakes, *Ann. Geofis., 9,* 1–15, 1956.

Iida, K., Earthquake magnitude, earthquake fault and source dimensions, *J. Earth Sci. Nagoya Univ., 13,* 115–132, 1965.

Kanamori, H., and J. J. Cipar, Focal processes of the great Chilean earthquake May 22, 1960, *Phys. Earth Planet. Interiors, 9,* 128–136, 1974.

King, C. Y., and L. Knopoff, A magnitude-energy relation for large earthquakes, *Bull. Seismol. Soc. Amer., 59,* 269–273, 1969.

Logan, J. M., T. Iwasaki, M. Friedman, and S. Kling, Experimental investigation of sliding friction in multilithologic specimens, *Eng. Geol. Case Hist. 9,* 55–67, 1972.

Mjachkin, V. F., G. A. Sobolev, N. A. Dolbilkina, V. N. Morozow, and V. B. Preobrozensy, The study of variations in geophysical fields near focal zones of Kamchatka, *Tectonophysics, 14,* 287–293, 1972.

Mogi, K., Earthquakes and fractures, *Tectonophysics, 5,* 35–55, 1967.

Mogi, K., Rock fracture and earthquake prediction, *J. Soc. Mater. Sci. Kyoto, 23,* 320–321, 1974.

Nason, R. D., Fault creep and earthquakes on the San Andreas fault, Proceedings of the Conference on Tectonic Problems of the San Andreas Fault System, *Stanford Univ. Publ. Univ. Ser. Geol. Sci., 13,* 275–285, 1973.

Nason, R. D., and D. Tocher, Anomalous fault slip rates before and after the April 1961 earthquakes near Hollister, California (abstract), *Eos Trans. AGU, 52,* 278, 1971.

Nur, A., Dilatancy, pore fluids, and premonitory variations of t_s/t_p travel times, *Bull. Seismol. Soc. Amer., 62,* 1217–1222, 1972.

Press, F., Dimensions of the source region for small shallow earthquakes, Proceedings of the VESIAC Conference on Shallow Source Mechanisms, *Rep. 7885-1-X,* pp. 155–163, Inst. of Sci. and Technol., Univ. of Mich., Ann Arbor, 1967.

Scholz, C. H., P. Molnar, and T. Johnson, Detailed studies of frictional sliding of granite and implications for the earthquake mechanism, *J. Geophys. Res., 77,* 6392–6406, 1972.

Scholz, C. H., L. R. Sykes, and Y. P. Aggarwal, Earthquake prediction: A physical basis, *Science, 181,* 803–810, 1973.

Stuart, W. D., Diffusionless dilatancy model for earthquake precursors, *Geophys. Res. Lett., 1,* 261–264, 1974.

Stuart, W. D., and M. J. S. Johnston, Anomalous tilt before three recent earthquakes, *Eos Trans. AGU, 56,* 400, 1975.

Thatcher, W., and T. C. Hanks, Source parameters of southern California earthquakes, *J. Geophys. Res., 78,* 8547–8576, 1973.

Tocher, D., Earthquake energy and ground breakage, *Bull. Seismol. Soc. Amer., 48,* 147–152, 1958.

Tocher, D., Creep on the San Andreas fault—Creep rate and related measurements at Vineyard, California, *Bull. Seismol. Soc. Amer., 50,* 396–404, 1960.

Tsubokawa, I., On relation between duration of crustal movement and magnitude of earthquake expected, *J. Geod. Soc. Jap., 15,* 75, 1969.

Weertman, J., Continuum distribution of dislocations on faults with finite friction, *Bull. Seismol. Soc. Amer., 54,* 1035–1058, 1964.

Whitcomb, J. H., J. D. Garmany, and D. L. Anderson, Earthquake prediction: Variation of seismic velocities before the San Fernando earthquake, *Science, 180,* 632, 1973.

Wyss, M., and J. Brune, Seismic moment, stress and source dimensions for earthquakes in the California-Nevada region, *J. Geophys. Res., 73,* 4681–4698, 1968.

Yerkes, R. F., and R. O. Castle, The Parkfield-Cholame, California earthquakes of June–August 1966: Engineering geology aspects, *U.S.Geol. Surv. Prof. Pap., 579,* 40–53, 1967.

(Received August 5, 1977;
revised February 10, 1978;
accepted March 17, 1978.)